Expanded View Figures

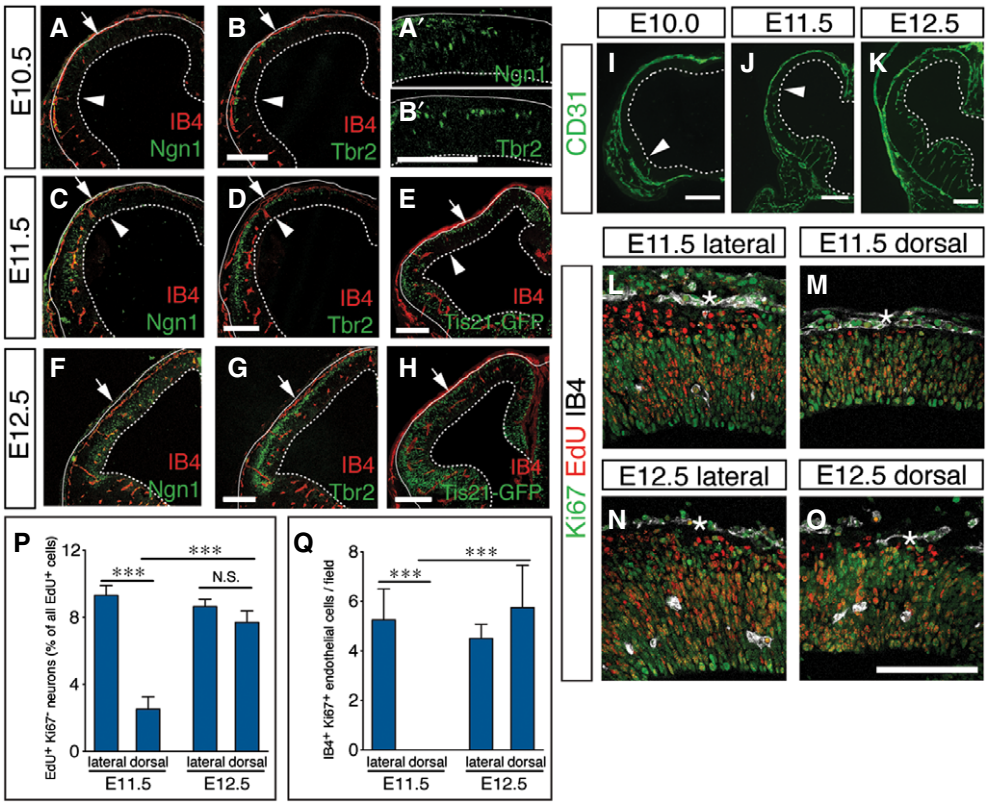

Figure EV1. Congruence of angiogenesis and NSC differentiation in the developing mouse cortex.

A–H Staining for isolectin B4 (IB4)$^+$ blood vessels and Ngn1$^+$ neurogenic NPCs (A, A', C, F), Tbr2$^+$ BPs (B, B', D, G) and *Tis21*-GFP$^+$ (E, H) neurogenic NPCs of the mouse cortex at E10.5 (A-B'), E11.5 (C-E), and E12.5 (F–H). Panels (A') and (B') show larger magnifications of the E10.5 cortex region above the vascular front. Arrows mark the border between lateral and dorsal cortex. Arrowheads in (A–E) denote the position of the vascular front.

I–K Immunostaining for CD31 in the cortex at E10.0 (I), E11.5 (J), and E12.5 (K). Arrowheads in (I) and (J) denote the position of the vascular front.

L–O Staining for Ki67 (green), EdU (red), and IB4 (white) in the lateral (L, N) and the dorsal (M, O) cortex at E11.5 (L, M) and E 12.5 (N, O), showing a temporo-spatial relationship between the appearance of isolectin B4$^+$ blood vessels in the parenchyma of lateral cortex from E11.5 (M) to E 12.5 (O) and the generation of Ki67$^-$ EdU$^+$ neurons. Asterisks indicate non-parenchymal, meningeal blood vessels.

P, Q Quantifications of the generation of Ki67$^-$ EdU$^+$ neurons (P) and the presence of IB4$^+$ Ki67$^+$ endothelial cells (Q) in the lateral and dorsal cortex shown in (L–M) (mean ± SEM; $N = 4$; ***$P < 0.001$).

Data information: Full and dotted lines indicate basal and apical boundaries of the cortex, respectively. N.S., not significant. Scale bars: 100 μm.

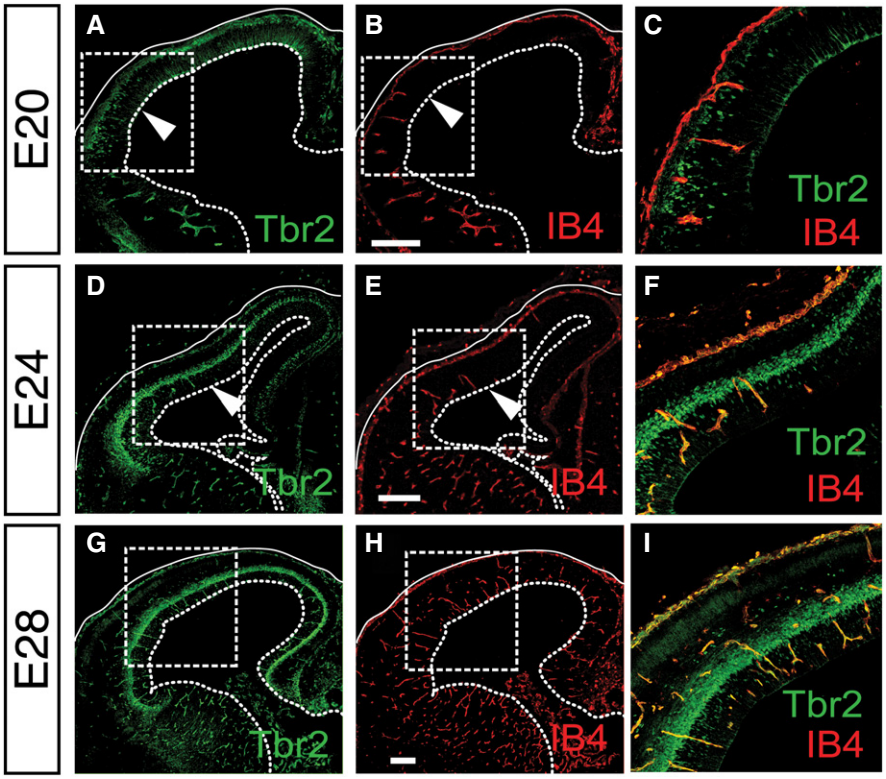

Figure EV2. Congruence of angiogenesis and NSC differentiation in the developing gyrencephalic ferret cortex.

A–I Stainings for Tbr2 (A, C, D, F, G, I) and isolectin B4 (IB4; B, C, E, F, H, I) in the ferret cortex at E20 (A–C), E24 (D–F) and E28 (G–I), showing induction of $Tbr2^+$ BPs specifically in the vascularized areas of the cortex. Panels (C, F, I) are merged magnifications of the boxed areas in (A) and (B), (D) and (E), or (G) and (H), respectively. Arrowheads in (A, B, D, E) denote the position of the vascular front. Full and dotted lines indicate basal and apical boundaries of the cortex, respectively. Scale bars: 200 μm.

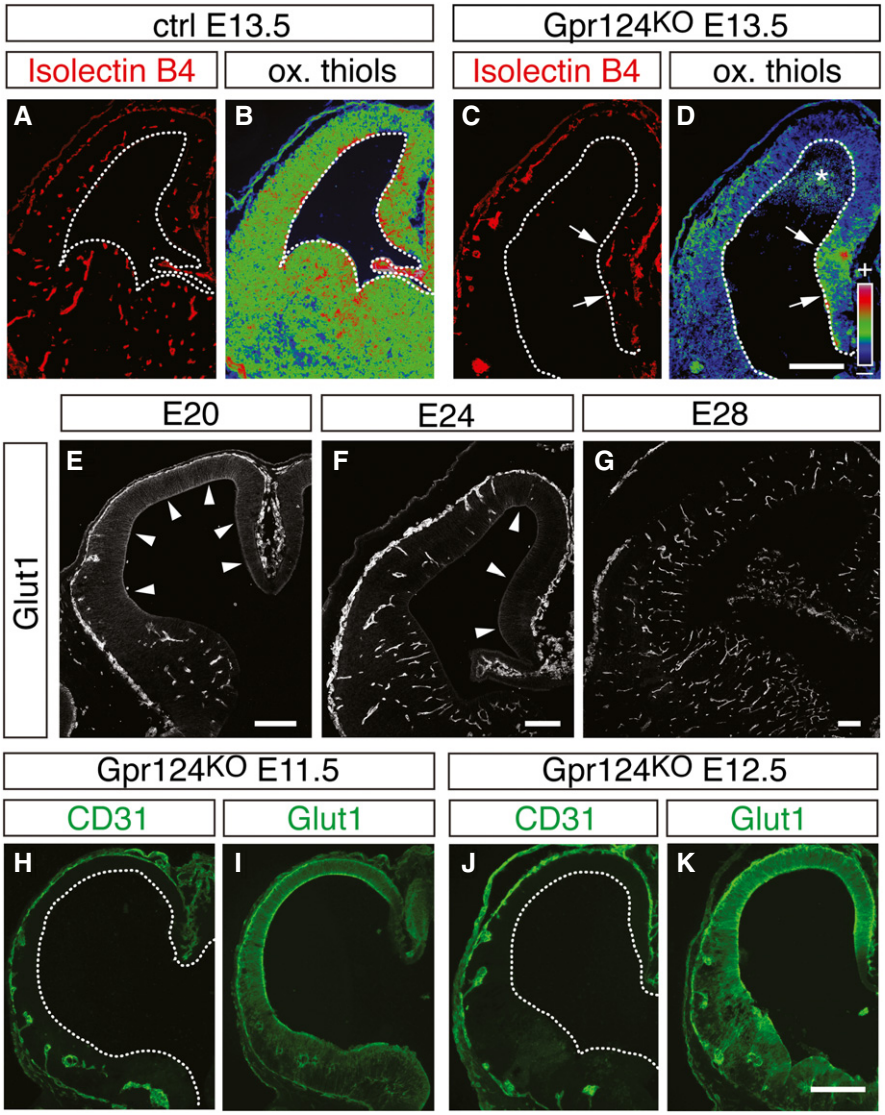

Figure EV3. Regulation of tissue oxygenation and neuroepithelial Glut1 expression in the Gpr124^{KO} mouse and ferret brain.

A–D Stainings for isolectin B4 (A, C) and oxidized thiols (B, D) in E13.5 control (A, B) and Gpr124^{KO} (C, D) cortices, showing reduced tissue oxygenation in the Gpr124^{KO} neocortex containing abnormal vessels. Note the more normal tissue oxygenation levels in the Gpr124^{KO} cortical hem containing normal vessels (C, D; arrows). The asterisk indicates hemorrhage of red blood in the mutant. Panels (B) and (D) are pseudocolor conversions of staining intensity (from low [purple] to high [red]).

E–G Immunostainings for Glut1 (white) in the developing ferret cortex at E20 (E), E24 (F), and E28 (G). Arrowheads point toward Glut1^{+} tissue.

H–K Immunostainings for CD31 (H, J) and Glut1 (I, K) in Gpr124^{KO} cortices, showing persistent high neuroepithelial Glut1 expression in the absence of functional CD31^{+} blood vessels at E11.5 (H, I) and at E12.5 (J, K).

Data information: Dotted lines indicate the apical boundary of the forebrain. Scale bars: 200 μm.

Figure EV4. Regulation of angiogenesis, cell survival, and hypoxia response element-dependent gene expression by HIF-1α.

A–D Stainings for TUNEL^{+} apoptotic cells (A, C) and CD31^{+} blood vessels (B, B', D, D') in E13.5 WT (A, B) and HIF-1α$^{CC-/-}$ (C, D) cortices. (B') and (D') are magnifications of the boxed areas in (B) and (D), respectively. Dashed lines indicate the ventral border of the dorsal cortex, where Cre is active and HIF-1α is deleted. The vascular area (% of total cortical area) is indicated (B, D; mean ± SEM; $N = 4$; $^{**}P < 0.01$).

E, F Immunostaining for CD31^{+} blood vessels in E13.5 WT (E) and HIF-1α$^{CC+/-}$ (F) cortices. The vascular area (% of total cortical area) is indicated (mean ± SEM; $N = 4$).

G Quantification of TUNEL^{+} cells in the cortex of E13.5 WT and HIF-1α$^{CC+/-}$ embryos, showing no significant changes of apoptosis (mean ± SEM; $N = 4$).

H–M Immunostainings for the deep layer markers Tbr1 (H, I), and Ctip2 (J, K) and the upper layer marker Brn2 (L, M) in P5 WT (H, J, L) and HIF-1α$^{CC+/-}$ (I, K, M) cortices.

N Quantification of Tbr1^{+}, Ctip2^{+}, or Brn2^{+} neurons within a 250-μm column of the cortex (mean ± SEM; $N = 4$).

O Quantification of hypoxia response element (HRE)-dependent luciferase activity in Neuro2A cells after transfection of 9xHRE::luciferase together with EGFP (control), wild-type HIF-1α (middle) or the transcriptionally impaired mutant HIF-1α-ΔC (right). A representative experiment is shown (mean ± SEM; $N = 3$; $^{***}P < 0.001$ compared to EGFP, $^{\#\#}P < 0.01$ compared to native HIF-1α).

Data information: Full and dotted lines in (A–M) indicate basal and apical boundaries of the cortex, respectively. A.U., arbitrary units; and N.S., not significant. Scale bars: 200 μm.

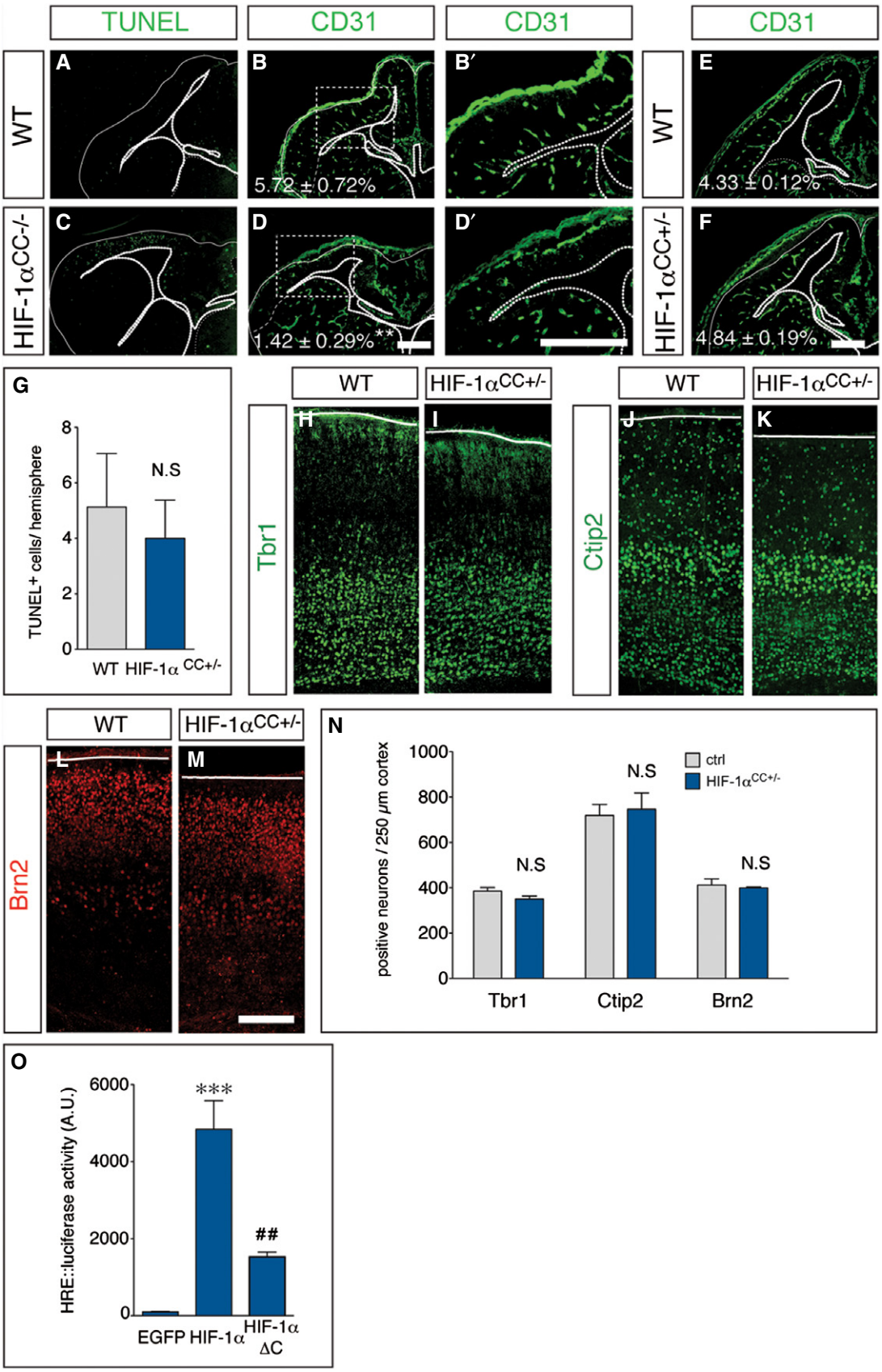

Figure EV4.

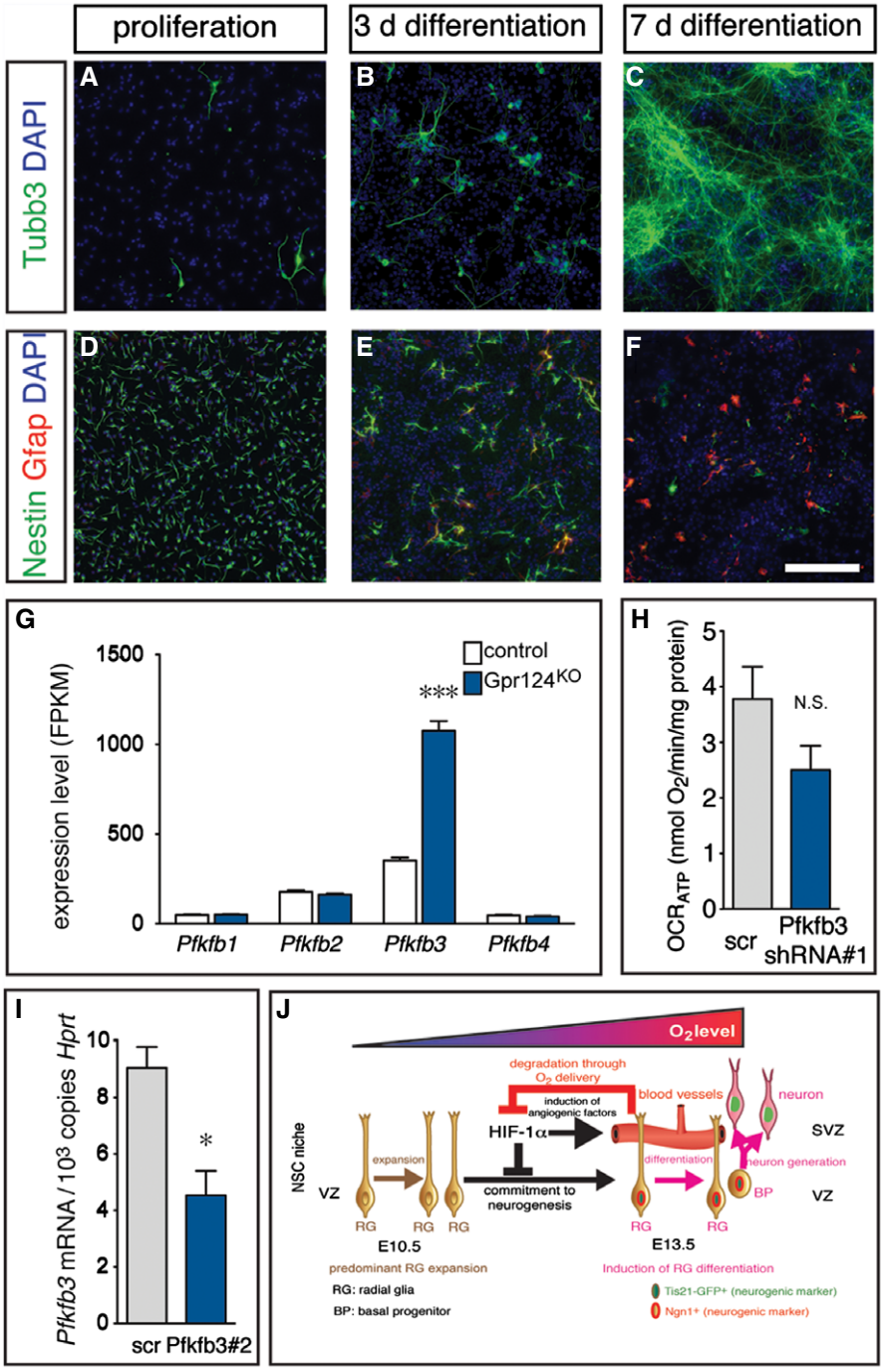

Figure EV5. NSC differentiation *in vitro* and regulation of PFKFB3 gene expression *in vivo* and by shRNA knockdown.

A–F Immunostainings for the neuronal marker Tubb3 (A–C; green), the NSC marker Nestin (D–F; green), the astrocyte marker Gfap (D–F; red) and counterstaining with DAPI (A–F; blue) in cultured NSCs derived from E13.5 cortex under proliferating conditions (A, D) or after 3 days of differentiation (B, E) and 7 days of differentiation (C, F). Note the beginning induction of neurogenesis and widespread loss of the NSC marker Nestin at 3 days of differentiation, thus demarcating the switch from expansion toward differentiation. Scale bar: 100 μm.

G Quantification of mRNA expression of Pfkfb isoforms *Pfkfb1*, *Pfkfb2*, *Pfkfb3*, and *Pfkfb4* in NSCs freshly sorted from control or $Gpr124^{KO}$ cortices by RNA sequencing (mean ± SEM; $N = 5$; $^{***}P < 0.001$). Note the strong and specific induction of *Pfkfb3* expression in NSCs from $Gpr124^{KO}$ cortices.

H Measurement of oxygen consumption rate used for mitochondrial ATP production (OCR_{ATP}) in proliferating NSCs, transduced with scr or Pfkfb3 shRNA#1, normalized to cellular protein content (mean ± SEM; $N = 3$; N.S., not significant).

I qRT–PCR analysis of *Pfkfb3* in cultured Neuro2a cells after transfection with plasmids encoding scr shRNA or Pfkfb3 shRNA#2 (mean ± SEM; $N = 3$; $^{*}P < 0.05$).

J Scheme depicting the model emerging from this study: RGs in the avascular cortical stem cell niche at E10.5 are exposed to low oxygen levels and mostly expand via symmetric divisions. Ingrowth of blood vessels in the niche until E13.5 increases oxygen levels in the niche and induces upregulation of neurogenic markers (Ngn1, *Tis21*-GFP) in RGs, leading to asymmetric divisions that generate neurogenesis-committed BPs and ultimately differentiated neurons. HIF-1α is initially active in the hypoxic niche at E13.5 and suppresses the commitment of RGs to neurogenesis. At the same time, HIF-1α also triggers vessel ingrowth, which increases oxygenation that in turn leads to the degradation of HIF-1α. Thus, a feedback loop emerges whereby HIF-1α ensures RG expansion, but at the same time also induces its own degradation via supply of oxygen by blood vessels to allow timely differentiation and proper brain development.